Gold Nanoparticles Generated by Electron Beam Lithography of Gold(I)−Thiolate Thin Films

Muriel K. Corbierre,[†] Jean Beerens,[‡] and R. Bruce Lennox*,[†]

Department of Chemistry and FQRNT Centre for Self-Assembled Chemical Structures, McGill University, 801 Sherbrooke Street West, Montréal, QC, H3A 2K6 Canada, and Département de Génie Electrique et Informatique, Université de Sherbrooke, 2500 Boul. de l'Université, Sherbrooke, QC, J1K 2R1 Canada

Received May 20, 2005. Revised Manuscript Received August 23, 2005

Patterned arrays of gold nanoparticles in two dimensions were prepared by the electron beam reduction and subsequent thermolysis of gold(I)−thiolate complexes on silicon surfaces. The array line widths are <50 nm and they are composed of small gold nanoparticles (average diameters from 2 to 4.5 nm). Variation in the electron beam dose allows for the variation of the interparticle distances in a given sample.

Introduction

The miniaturization of optical and electrical devices for applications in information technology requires a capability to generate metal nanopatterns on surfaces. Typical feature sizes in the microelectronics industry were in the range 90−180 nm in 2001 and are predicted to be below 35 nm by 2016.[1] The specific conductance[2,3] and optical properties[4−9] of such metallic nanopatterns make them of particular interest for future industrial applications. For example, two-dimensional (2D) arrays of metal nanoparticles have been shown to exhibit an insulator-to-metal transition when the particle−particle distance becomes less than a critical distance.[10−12] Optical properties of importance include the surface plasmon enhanced nonlinear response signal in gold nanoparticles.[4] Gold nanoparticles or nanowires have also been molecularly linked with thiol-endcapped conducting molecules in order to create conductive molecular electronic networks.[13,14] Finally, gold nanomaterials have been demonstrated to have applications in biomedical research[15] and catalysis.[16]

Many research groups are involved in the solution syntheses of Au nanoparticles.[16,17] Once the nanoparticles are prepared in solution, the challenge is to assemble them into well-defined lattices or superlattices on a surface.[16,17] Many techniques are currently being used for the generation of metallic nanostructures on surfaces. Of note is the example where electron beam writing on functionalized surfaces produces chemically activated nanopatterns. The result is nanometer-scale patterns with a different chemical speciation than the unexposed parts of the surface.[18−20] These nanopatterns are then used to adsorb citrate-passivated gold nanoparticles in a selective fashion due to the intrinsic difference in affinities for the surface functional groups.[20] Lines of adsorbed nanoparticles with sub-200 nm widths have been reported.

Direct electron beam writing (DEBW) on thin films of pre-made thiol-stabilized or phosphine-stabilized gold nanoparticles has also been reported.[21−27] These films are typically formed at an air/water interface using a Langmuir film

* To whom correspondence should be addressed. E-mail: Bruce.Lennox@mcgill.ca.
[†] McGill University.
[‡] Université de Sherbrooke.

(1) Palmer, R. E. *Surf. Interface Anal.* **2002**, *34*, 3−9.
(2) Li, C. Z.; Sha, H.; Tao, N. J. *Phys. Rev. B* **1998**, *58*, 6775−6778.
(3) Bietsch, A.; Schneider, M. A.; Welland, M. E.; Michel, B. *J. Vac. Sci. Technol. B* **2000**, *18*, 1160−1170.
(4) Antoine, R.; Brevet, P. F.; Girault, H. H.; Bethell, D.; Schiffrin, D. J. *J. Chem. Soc., Chem. Commun.* **1997**, 1901−1902.
(5) Murray, C. B.; Kagan, C. R.; Bawendi, M. G. *Annu. Rev. Mater. Sci.* **2000**, *30*, 545−610.
(6) Maier, S. A.; Brongersma, M. L.; Kik, P. G.; Meltzer, S.; Requicha, A. A. G.; Atwater, H. A. *Adv. Mater.* **2001**, *13*, 1501−1505.
(7) Maier, S. A.; Kik, P. G.; Atwater, H. A.; Meltzer, S.; Harel, E.; Koel, B. E.; Requicha, A. A. G. *Nat. Mater.* **2003**, *2*, 229−232, and references therein.
(8) Bruzzone, S.; Arrighini, G. P.; Guidotti, C. *Chem. Phys.* **2003**, *291*, 125−140.
(9) Schider, G.; Krenn, J. R.; Hohenau, A.; Ditlbacher, H.; Leitner, A.; Aussenegg, F. R.; Schaich, W. L.; Puscasu, L.; Monacelli, B.; Boreman, G. *Phys. Rev. B* **2003**, *68*, 155427.
(10) Collier, C. P.; Saykally, R. J.; Shiang, J. J.; Henrichs, S. E.; Heath, J. R. *Science* **1997**, *277*, 1978−1981.
(11) Shiang, J. J.; Heath, J. R.; Collier, C. P.; Saykally, R. J. *J. Phys. Chem. B* **1998**, *102*, 3425−3430.
(12) Medeiro-Ribeiro, G.; Ohlberg, D. A. A.; Williams, R. S.; Heath, J. R. *Phys. Rev. B* **1999**, *59*, 1633−1636.
(13) Andres, R. P.; Bielefeld, J. D.; Henderson, J. I.; Janes, D. B.; Kolagunta, V. R.; Kubiak, C. P.; Mahoney, W. J.; Osifchin, R. G. *Science* **1996**, *273*, 1690−1693.
(14) Hassenkam, T.; Moth-Poulsen, K.; Stuhr-Hansen, N.; Nørgaard, K.; Kabir, M. S.; Bjørnholm, T. *Nano Lett.* **2004**, *4*, 19−22.
(15) Zhang, H.; Li, Z.; Mirkin, C. A. *Adv. Mater.* **2002**, *14*, 1472−1474.
(16) Daniel, M.-C.; Astruc, D. *Chem. Rev.* **2004**, *104*, 293−346.
(17) Shipway, A. N.; Katz, E.; Willner, I. *ChemPhysChem* **2000**, *1*, 18−52.
(18) Gölzhäuser, A.; Eck, W.; Geyer, W.; Stadler, V.; Weimann, T.; Hinze, P.; Grunze, M. *Adv. Mater.* **2001**, *13*, 806−809.
(19) Wouters, D.; Schubert, U. S. *Angew. Chem., Int. Ed.* **2004**, *43*, 2480−2495; *Angew. Chem.* **2004**, *116*, 2534−2550.
(20) Mendes, P. M.; Jacke, S.; Critchley, K.; Plaza, J.; Chen, Y.; Nikitin, K.; Palmer, R. E.; Preece, J. A.; Evans, S. D.; Fitzmaurice, D. *Langmuir* **2004**, *20*, 3766−3768.
(21) Clarke, L.; Wybourne, M. N.; Yan, M.; Cai, S. X.; Keana, J. F. W. *Appl. Phys. Lett.* **1997**, *71*, 617−619.
(22) Bedson, T. R.; Nellist, P. D.; Palmer, R. E.; Wilcoxon, J. P. *Microelectron. Eng.* **2000**, *53*, 187−190.
(23) Bedson, T. R.; Palmer, R. E.; Jenkins, T. E.; Hayton, D. J.; Wilcoxon, J. P. *Appl. Phys. Lett.* **2001**, *78*, 1921−1923.

10.1021/cm051085b CCC: $30.25
Published on Web 10/04/2005

balance and then transferred onto a solid substrate.[26] Alternatively, films have been formed from solutions of nanoparticles via drop-casting or spin-coating onto a substrate.[21−25,27] There are conflicting opinions as to what effect the electron beam has on the nanoparticle films. The narrowest line width thus far obtained from the DEBW technique is 26 nm.[22,23]

Although narrow lines of gold nanoparticles have been achieved by the DEBW technique, it remains a complicated, multistep process (i.e., synthesis and cleaning of gold nanoparticles, preparation of a monolayer of nanoparticles on a surface, beam exposure, and solvent wash). To take advantage of the plasmon resonance properties of metal quantum dots, it is of interest to be able to tune the inter-nanoparticle distances within one sample. This is not possible with the DEBW method.

Electron beam techniques have considerable potential for the creation of small features compared to conventional techniques such as photolithography. Electron beam lithography systems routinely use beam sizes smaller than 5 nm, which in principle allows for very small features. The formation of metal nanowires and nanodots by conventional electron beam lithography consists of five steps: (i) an organic resist is spin-coated onto a substrate, (ii) the pattern is formed using the electron beam, (iii) the sample is developed in a solvent bath, (iv) metal is evaporated on the substrate, and (v) the excess metal is lifted off. Small gold nanofeatures are obtained in this process (e.g., dots with 15−35 nm diameters, with edge-to-edge distances of 50 nm, or rods with 50 nm width).[3,28] Because of proximity effects, it can be challenging to make nanodots that are very close to one another (i.e., <50 nm) by this technique. Moreover, the more steps there are in the process, the more likely it is that defects arise in the resulting nanostructures. It is therefore of interest to develop new electron beam processes that involve fewer steps.

Electron beam writing on surfaces of gold "compounds" have been reported.[29,30] In the work by Fraser et al.,[29] gold oxide and gold bromide are deposited onto glass substrates via sputtering gold atoms through gaseous oxygen or bromine environment. Following electron beam exposure, the substrates are developed in hydrochloric acid or water. The resulting gold pattern features are on the order of 200 nm wide. This technically demanding fabrication process requires in situ formation of gold oxide or bromide and subsequent deposition onto the substrates. In another approach, Craighead et al.[30] spin-coated Engelhard gold solutions (from Engelhard-CLAL Inc.) onto various substrates and exposed the resulting solvent-free film to an electron beam. The precise nature of the gold solutions used ("a gold mercaptide with organic binders, and a small amount of other ingredients to promote adhesion")[30] is undisclosed, however. The resulting patterns were developed in methylene chloride in order to remove unexposed material and then pyrolyzed in air at 450 °C to remove any organic material remaining in the exposed regions. The features obtained are typically larger than 250 nm.

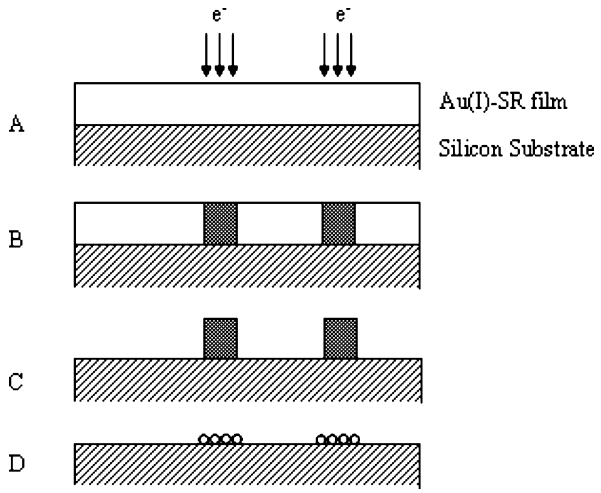

Figure 1. (A) Spin-coating and electron beam exposure on the Au(I)−SR film; (B) the pattern after exposure; (C) the pattern after development; (D) the pattern after thermolysis.

In related work, Russell et al.[31] used electron beam writing of palladium acetate films to obtain 100 nm wide Pd lines containing a Pd/C atomic ratio of 1. Finally, Manners et al.[32] produced 72 nm wide bars consisting of heterogeneous ferromagnetic clusters by electron beam writing on their Fe/Co organometallic polymer films.

In this paper, we report the reduction of Au(I) polymer complexes (in the form of solid, homogeneous thin films), using an electron beam lithography (EBL) instrument. EBL studies were concentrated on a gold(I)−polystyrenethiol (Au(I)−PS_{19}) complex, although preliminary experiments show that similar results can be obtained with other Au(I)−thiolate complexes such as Au(I)−thiocholesterol. Briefly, the technique consists of spin-coating a Au(I)−thiolate film onto a silicon surface. Following the formation of nanofeatures by EBL, the substrate is "developed" in an organic solvent. The developing process removes the unexposed regions of the film. The sample is then thermolyzed for a few minutes to remove the organic phase trapped within the nanofeatures formed. Figure 1 summarizes the fabrication steps. EBL of Au(I)−thiolate thin films provides reproducible nanofeatures in the sub-50 nm region consisting of small, monodisperse gold nanoparticles (average diameters vary between 2 and 4.5 nm depending on the conditions). This work differs from the previous studies mentioned above in that (i) a new polymeric material was used as the nanoparticle precursor, (ii) this precursor material is fully characterized, (iii) the precursor material spreads easily on substrates to

(24) Bedson, T. R.; Palmer, R. E.; Wilcoxon, J. P. *Appl. Phys. Lett.* **2001**, *78*, 2061−2063.
(25) Griffith, S.; Mondol, M.; Kong, D. S.; Jacobson, J. M. *J. Vac. Sci. Technol. B* **2002**, *20*, 2768−2772.
(26) Werts, M. H. V.; Lambert, M.; Bourgoin, J.-P.; Brust, M. *Nano Lett.* **2002**, *2*, 43−47.
(27) Lin, X. M.; Parthasarathy, R.; Jaeger, H. M. *Appl. Phys. Lett.* **2001**, *78*, 1915−1917.
(28) Niklasson, G. A.; Craighead, H. G. *Thin Solid Films* **1985**, *125*, 165−170.
(29) Fraser, D. B.; Kammlott, G. W. U.S. Patent US 4072768, 1978.
(30) Craighead, H. G.; Schiavone, L. M. *Appl. Phys. Lett.* **1986**, *48*, 1748−1750.
(31) Stark, T. J.; Mayer, T. M.; Griffis, D. P.; Russell, P. E. *J. Vac. Sci. Technol. B* **1991**, *9*, 3475−3478.
(32) Clendenning, S. B.; Aouba, S.; Rayat, M. S.; Grozea, D.; Sorge, J. B.; Brodersen, P. M.; Sodhi, R. N. S.; Lu, Z.-H.; Yip, C. M.; Freeman, M. R.; Ruda, H. E.; Manners, I. *Adv. Mater.* **2004**, *16*, 215−219.

provide uniform films, (iv) the resulting gold nanoparticles are located in well-defined sub-50 nm regions, and (v) variation in the electron dose within a given sample is shown to allow for tuning the interparticle distances in the patterns.

Experimental Section

Au(I)−Thiolate Complexes. PS_{19}−SH (a thiol-terminated polystyrene (PS) chain with 19 styrene repeat units) was synthesized by anionic polymerization, as described previously.[33] Purification was monitored by ^{1}H NMR using deuterated chloroform as a solvent. Thiocholesterol, thiodiglycol, and $HAuCl_4 \cdot 3H_2O$ were purchased from Sigma-Aldrich and used as received. The Au(I)−PS_{19} and Au(I)−thiocholesterol complexes were synthesized following the thiodiglycol procedure.[34] Briefly, 200 mg of $HAuCl_4 \cdot 3H_2O$ (FW = 393.8 g/mol) was dissolved in 10 mL of MilliQ water (Millipore). The solution was cooled in an ice bath. 150 μL of thiodiglycol (FW = 122.19 g/mol, d = 1.221 g/cm^3) was then added over an hour, resulting in a clear colorless solution; 964 mg of PS_{19}−SH (Mn = 1900 g/mol) dissolved in 20 mL of chloroform was added over an hour and a half, and the solution was stirred for another hour. The cloudy chloroform phase was separated from the aqueous phase, and the chloroform was rotovaped to dryness. The Au(I)−PS_{19} complex was then dissolved in 2−3 mL of toluene and precipitated by slowly adding it to a stirred water/methanol mixture. Au(I)−PS_{19} was then vacuum-filtered and dried under vacuum. The gold(I)−thiolates were characterized by thermogravimetric analysis, solution ^{1}H and ^{13}C NMR, and X-ray photoelectron spectroscopy. Detailed synthetic procedures and characterizations are described elsewhere.[35]

Thin Film Preparation. The substrates for thin film preparation were silicon [111] (Si) substrates (SiliconQuest, USA). The Si wafers were cleaned in a nitric acid bath, rinsed with MilliQ water, sonicated in ethanol for 1 min, rinsed with chloroform, and finally rinsed with anhydrous ethanol. The Si wafers were then dried under a stream of dry N_2 gas and were used immediately. The Au(I)−thiocholesterol complex was dissolved in chloroform, and the dilute solution was drop-cast on a water surface. After evaporation of the solvent (ca. 10 min), the thin films were transferred onto the Si wafers. The Au(I)−PS_{19} thin films were prepared by spin-coating toluene solutions of various concentrations on Si wafers. A Laurell benchtop spin-coater (Laurell Technologies Corp., USA) was used, with speeds ranging from 4000 to 6000 rpm. The thickness of the spin-coated films was estimated by AFM imaging of narrow scratches made in the overlayer film.

Electron Beam Lithography. Both the electron beam lithography and SEM observations were performed on field-emission gun scanning electron microscopes (FEG-SEM) (Leo 1500 series equipped with the nanometer pattern generation system NPGS, from JC Nabity Lithography systems). During electron beam lithography, the FEG-SEM was set at an acceleration voltage of 20 kV and a beam current of 425 pA. Under these conditions, the electron beam diameter is less than 2 nm. A dose-matrix experiment was conducted for each of a series of initial Au(I)−thiolate film thicknesses. In some cases, isolated lines were made in the resist using single-pass exposure to the electron beam. In other cases, finite areas were exposed on the sample (closed polygons of various shapes, e.g. triangles, lines of finite width or rectangles) by sweeping the electron beam over the area. These conditions can be easily distinguished, based on the units used to characterize the dose received by the sample. Either linear doses (expressed in nC/cm) or surface doses (mC/cm^2) are cited. FEG-SEM observations were made in the backscattered electron mode, using an "in-lens" detector.

Following pattern writing in the electron beam, the wafers were immersed for 1 min in a chloroform bath at 20 °C and were then dried in a stream of nitrogen gas. The developing process removes the unexposed parts of the thin film, leaving only the exposed regions on the surface. Some of the patterns (depending on their size) were observed by optical microscopy after development. The final step of the process was the removal of the residual organic material (from the initial Au(I)−thiolate film) remaining in the exposed patterns by thermolysis. This was effected by heating the wafers at 400 °C for 10 min in a nitrogen flow.

The exposed regions were observed by FEG-SEM before and after the heating step. The heights of the patterns before and after this thermolysis step were also examined using contact mode AFM (AutoProbe CP, Park Scientific Instruments, USA) with silicon tips (Microlevers, Veeco Metrology LLC). XPS (VG ESCALAB 220i-XL spectrometer) was also performed on the final nanopatterns in order to determine the chemical composition of the gold nanoparticles.

Results and Discussion

We first identified the potential of using e-beam irradiation to make nanoparticles from our polymeric gold complexes by the e-beam in a transmission electron microscope (TEM).[36] In the TEM environment (a JEOL JEM-2000 FX TEM at an acceleration voltage of 80 kV), nanoparticle growth was observed with increasing exposure time at a constant beam intensity on a Au(I)−thiocholesterol film deposited on a carbon-coated grid.[36] The nanoparticle diameters increased from 1.8 (0.3) nm for 1 min exposure up to 3.4 (0.7) nm for 9 min. As per a very recent report,[37] the impinging e-beam clearly leads to in situ formation of gold nanoparticles. However, important parameters such as the electron dose and film conditions (thickness and uniformity of the Au(I)−thiolate film) are very difficult to control in the TEM environment. We thus turned to the electron beam lithography (EBL) experiment to explore its potential to convert these gold complexes into nanoparticles in a controlled fashion.

Most EBL experiments were performed on spin-coated films of Au(I)−PS_{19} deposited on silicon wafers coated with a native silicon oxide layer. The initial thickness of the Au(I)−PS_{19} film ranged from ca. 50 to ca. 900 nm. For comparison purposes, some patterns formed were examined before the thermolysis step by SEM and AFM. Because we did not find adequate spin-coating conditions for the Au(I)−thiocholesterol complexes, films were made from this precursor by drop-casting Au(I)−thiocholesterol solutions on water, followed by transfer to the silicon substrates. This method, however, generates inhomogeneous film thickness. Preliminary lithography experiments were performed on Au(I)−thiocholesterol films prepared in this fashion. Nanopatterns were indeed obtained, but the uneven thickness of

(33) Corbierre, M. K.; Cameron, N. S.; Lennox, R. B. *Langmuir* **2004**, *20*, 2867−2873.
(34) Al-Sa'ady, A. K.; McAuliffe, C. A.; Parish, R. V.; Sandbank, J. A. *Inorg. Synth.* **1985**, *23*, 191.
(35) Corbierre, M. K.; Lennox, R. B. *Chem. Mater.* **2005**, in press.
(36) Corbierre, M. K. Ph.D. Dissertation, McGill University, 2004.
(37) Kim, J.-U.; Cha, S.-H.; Shin, K.; Jho, J. Y.; Lee, J.-C. *J. Am. Chem. Soc.* **2005**, *127*, 9962−9963.

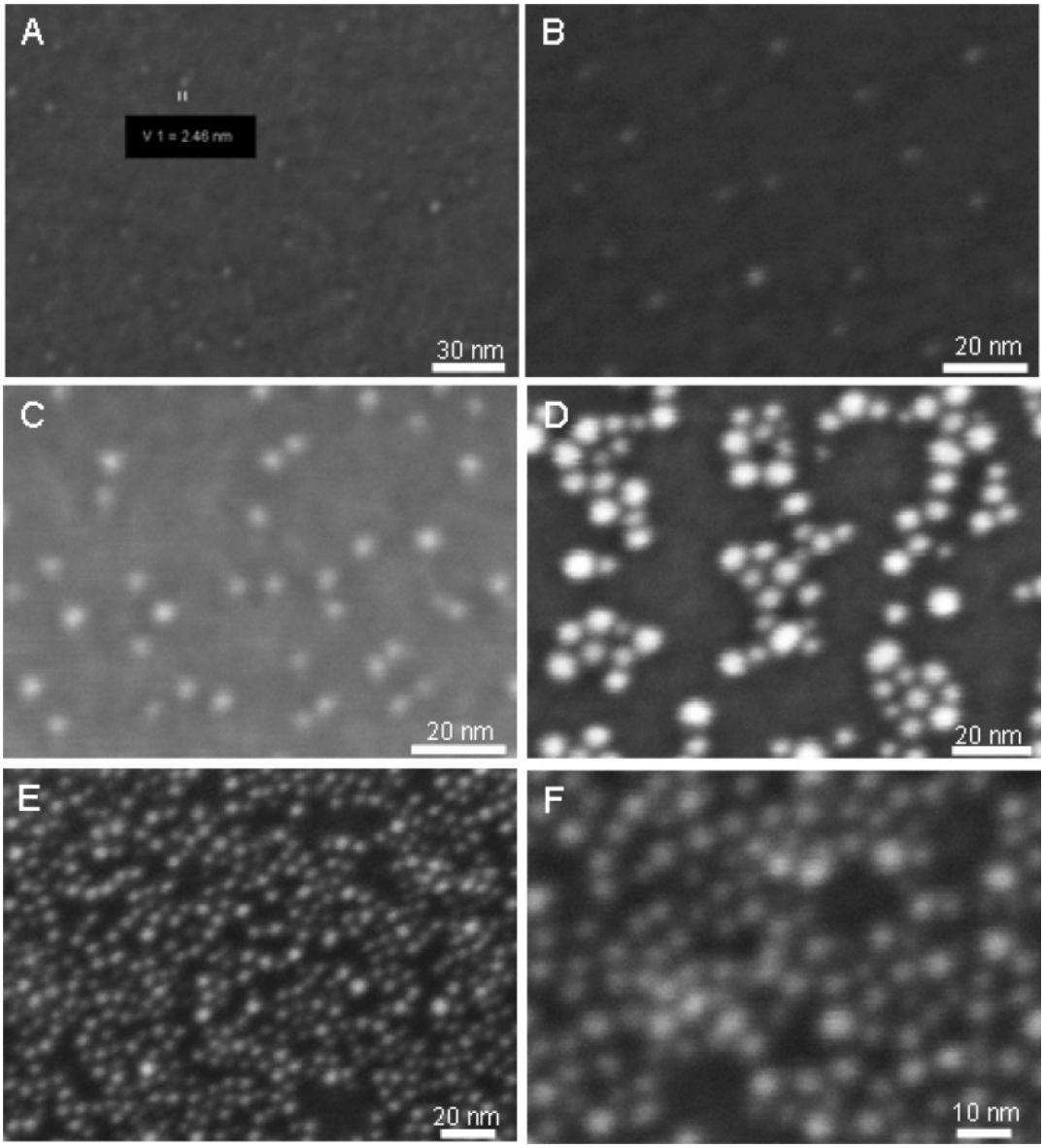

Figure 2. SEM images displaying the effect of electron beam dose on gold nanoparticle size and number density formed from a 110 nm thick film of Au(I)−PS_{19}, post-thermolysis. Beam doses: (A) 0.5 mC/cm^2; (B) 1.0 mC/cm^2; (C) 2.6 mC/cm^2; (D) 4.9 mC/cm^2; (E) 7.9 mC/cm^2; (F) 9.8 mC/cm^2.

the initial film led us to concentrate on the Au(I)−PS_{19} system.

The electron beam dose has a considerable effect on a Au(I)−PS_{19} film of a given thickness. A range of doses (from 0.5 to 30 mC/cm^2) was tested on a 38 × 28 μm surface of the 110 nm thick film. Gold nanoparticles are obtained using doses between 0.5 and 9.8 mC/cm^2, with a high degree of monodispersity within a given sample (Figure 2). The variation in electron dose has a pronounced effect on the number of nanoparticles per unit surface area and only a slight effect on the final nanoparticle diameter. The Au surface coverage percentage values are calculated from the FEG-SEM images. We assume, based on our AFM thickness measurements, that the particles are spherical because the nanoparticle thicknesses match the diameters. The dispersion in the diameter values ranges from 0.4 to 1.5 nm, depending on the dose used. For the lowest surface dose studied, very few gold nanoparticles are apparent after the thermolysis step (less than 1% surface coverage) and they are quite small (ca. 2 nm diameter). As shown in Table 1, as the dose is incrementally increased to 9.8 mC/cm^2, the coverage increases to 20%. The nanoparticle average diameters do not correlate with dose but remain in the 2−4.5 nm range. When transposed into a volume of Au imaged on the surface (and assuming that the gold nanoparticles are spherical), the 9.8 mC/cm^2 exposure yields nanoparticles whose Au content equals that of the initial quantity of Au(I)−PS_{19} deposited

Table 1. Nanoparticle Dimensions and Surface Coverage for Varying Electron Doses

dose (mC/cm^2)	nanoparticle diameters [a] (nm)	surface coverage [b] (%)
0.5	ca. 2 [c]	<1
1	2.5 (0.4)	1
2.6	2.8 (0.4)	5
4.9	4.5 (1.5)	13
7.9	3.0 (0.7)	15
9.8	3.5 (0.9)	20

[a] From FEG-SEM images, with the standard deviations in parentheses. [b] From FEG-SEM images, assuming spherical gold nanoparticles. [c] No distribution measured because diameters are too small.

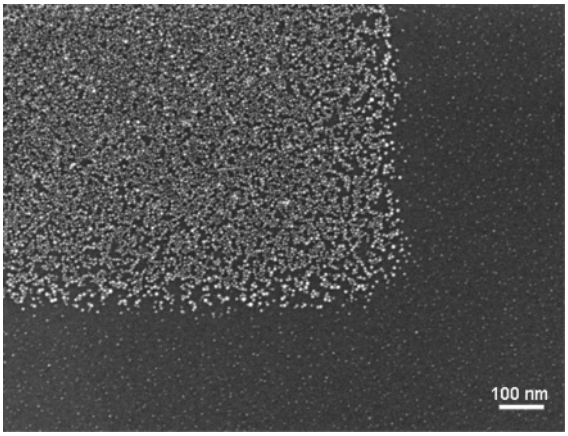

Figure 3. Variation of electron beam dose on the Au(I)−PS_{19} film (110 nm thick), after thermolysis. The top left region of the SEM image corresponds to a dose of 9.8 mC/cm^2 (resulting nanoparticle density = 18.6 × 10^{11} particles/cm^2), while the remainder of the image corresponds to a dose of 1.0 mC/cm^2 (resulting nanoparticle density = 2.6 × 10^{11} particles/cm^2).

on the surface.[38] Above a 10 mC/cm^2 dose, significant cross-linking of the organic component occurs under the electron beam, and not all of the organic material is completely removed in the 110 nm thick film using thermolysis conditions of 400 °C, 10 min, N_2.

The striking effect of electron dose on the formation of nanoparticles (both surface coverage and size) is apparent in Figure 3. The square on the top left of the image experienced an electron beam dose of 10 mC/cm^2, while the remainder of the sample was subjected to a 1 mC/cm^2 dose. Variation of the gold nanoparticle surface density (and therefore the interparticle distances) is clearly accessible by simply varying the electron beam dose. This is important as there are few effective means to control the interparticle distances between gold nanoparticles adsorbed on chemically modified lines. Natan et al.,[39] for example, reported a kinetic control of citrate-stabilized gold nanoparticle spacings on thiol-functionalized surface as a function of the immersion time of the substrates in the nanoparticle solutions. However, quite long immersion times are necessary to reach significant surface coverage (e.g., 3 days of immersion to obtain 1.8 × 10^{11} particles/cm^2).

The nanoparticles formed after thermolysis of the sample are composed of elemental gold, as determined by XPS measurements on a large array of nanoparticles. Sulfur was not detected by XPS. The formation mechanism of the gold nanoparticles in our technique is not yet fully understood. Preliminary HR-TEM results suggest that most of the gold nanoparticle growth occurs during the thermolysis step and that small gold nuclei are probably formed during the e-beam reduction step of the Au(I)−thiolates. Significantly, no gold nanoparticles are observed within 50 nm thick developed patterns prepared on a TEM grid, when no thermolysis step is undertaken.

(38) TGA results and density values of 1.05 g/cm^3 for PS and 19.3 g/cm^3 for Au combine to yield a volume fraction of PS_{19}/Au of 187/1 in the Au(I)−PS_{19} complex.

(39) Grabar, K. C.; Smith, P. C.; Musick, M. D.; Davis, J. A.; Walter, D. G.; Jackson, M. A.; Guthrie, A. P.; Natan, M. J. *J. Am. Chem. Soc.* **1996**, *118*, 1148−1153.

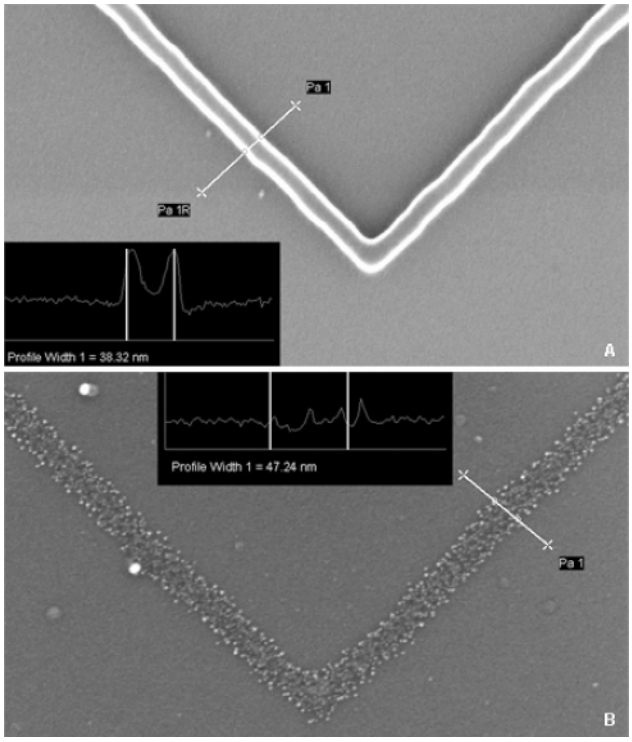

Figure 4. Patterns obtained from a 50 nm thick Au(I)−PS_{19} film using a beam dose of 140 nC/cm: (A) pre-thermolysis; (B) post-thermolysis. The resulting line widths (inset) on the SEM images are 38.3 and 47.2 nm, respectively.

Lines 40 nm wide were drawn onto the 50 nm thick Au(I)−PS_{19} film (Figure 4A). A range of linear doses from 100 to 160 nC/cm was used. The resulting lines are relatively straight and the 90° angle feature is well-reproduced. There is no significant variation in the resulting features for the different electron doses used. The height of the lines after developing (but before thermolysis) was measured by AFM to be ca. 50 nm. This is consistent with the initial thickness of the gold(I)−thiolate polymer film. After thermolysis, the line widths are slightly increased by 7 nm but the overall line shape is intact. Compared to the 110 nm thick Au(I)−PS_{19} film, the 50 nm thick film yields much narrower lines after thermolysis whereas the line widths before thermolysis had similar values for both film thicknesses. It is thus likely that the 110 nm thick lines collapsed to a greater extent than the 50 nm thick ones in the thermolysis step, yielding larger line widths for the former. These lines consist of monolayers of distinct nanoparticles, as per SEM observation (Figure 4B) and AFM-measured heights (between 5 and 8 nm). Figure 5 shows an example of AFM imaging on a gold nanoparticle linear array written at a dose of 25 mC/cm^2. It is noteworthy that the line widths are highly reproducible between several independently prepared samples. The line width values are likely to be further reduced by using different substrate materials, leading to fewer numbers of back-scattered electrons.[24]

Electron beam writing was also performed on a much thicker (900 nm) Au(I)−PS_{19} film. Electron beam linear doses (between 100 and 160 nC/cm) appear to cause the 50 nm (wide) × 900 nm (high) lines to collapse on their side during pattern development. Indeed, AFM and SEM reveal

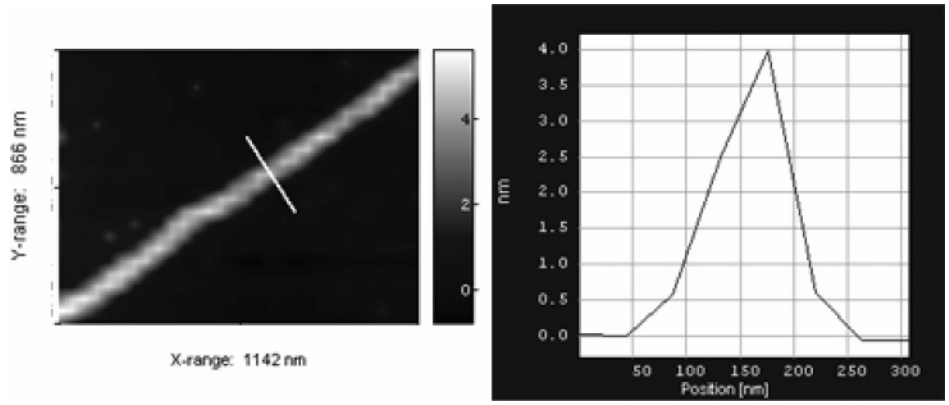

Figure 5. AFM image of a line of nanoparticles drawn using a beam dose of 25 mC/ m^2 on a 50 nm thick film of Au−PS_{19}. The vertical scale (RHS) on the AFM image is in nanometers. The accompanying plot is the line scan (height) associated with the white line on the AFM image.

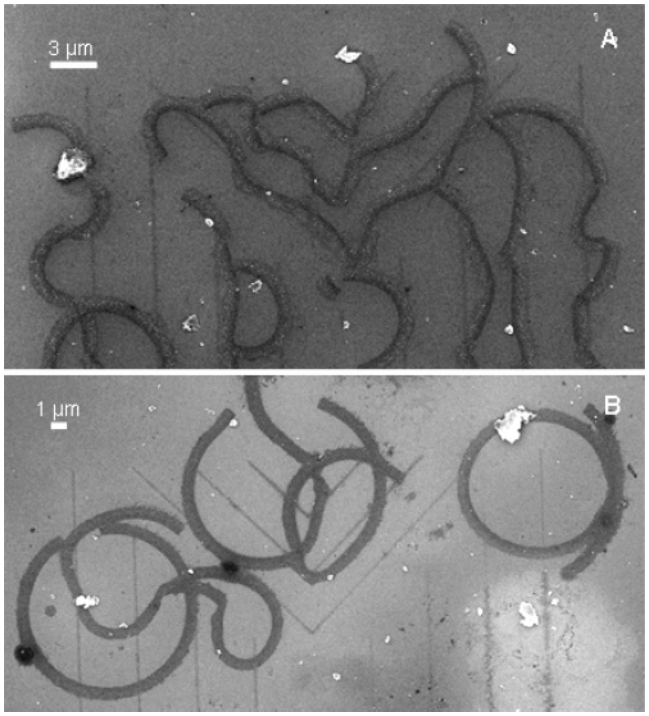

Figure 6. SEM images showing collapsed patterns formed from a 900 nm thick Au(I)−PS_{19} film, post-thermolysis, using a beam dose of (A) 160 nC/cm and (B) 120 nC/cm.

50 nm high and 900 nm wide "ribbons" in various shapes, some still attached to the substrate at their initial position (Figure 6A). Others are folded in circles next to their initial position on the substrate (Figure 6B). After thermolysis, the "ribbons" consist of monolayers of gold nanoparticles (6 nm high). Lines with a smaller initial thickness-to-width ratio (900/500 nm) written with 50 mC/cm^2 do not collapse upon development. The thicknesses after thermolysis suggest that most of the organic phase is still present.

Conclusions

The preparation of novel sub-50 nm patterns composed of ca. 3 nm arrayed gold nanoparticles is reported. Electron beam lithography of thin films of Au(I)−thiolate complexes is used to form these nanoparticles. The nanopattern features are highly reproducible between independently prepared samples and they are highly consistent with the target features (e.g., 90° elbows). Our preliminary study of the effect of the Au(I)−thiolate film thickness suggests that the target line widths are better achieved with the thinner, 50 nm Au(I)−PS_{19} film, following the thermolysis step. The nanoparticle diameters are in the range 2−6 nm, and average diameters are in the range 2−4.5 nm. Variation of the electron dose allows for control of the resulting interparticle distances. Other techniques do not allow variations in the interparticle distances on a given sample.

In future experiments, other types of substrates will be used in order to vary the quantity of back-scattered electrons, which is known to affect the optimal line widths achievable on a given resin layer composition.[24] Finally, transport properties of the nanoparticle arrays are of interest, due to the position/packing features of the nanoparticles in the arrays.[7,10]

Acknowledgment. The authors thank Prof. J. Beauvais for his support. Funding was provided by NanoQuébec, FQRNT, and NSERC.

CM051085B